Hong-Ou-Mandel interference between independent III-V on silicon waveguide integrated lasers

C. Agnesi[1], B. Da Lio[2], D. Cozzolino[2], L. Cardi[2], B. Ben Badir[3], K. Hassan[3], A. Della Frera[4], A. Ruggeri[4], A. Giudice[4], G. Vallone[1], P. Villoresi[1], A. Tosi[5], K. Rottwitt[2], Y. Ding[2], and D. Bacco[2,*]

[1] Dipartimento di Ingegneria dell'Informazione, Università degli Studi di Padova, via Gradenigo 6B, 35131 Padova, Italy
[2] CoE SPOC, DTU Fotonik, Dep. Photonics Eng., Technical University of Denmark, Ørsteds Plads 340, 2800 Kgs. Lyngby, Denmark
[3] CEA-Leti, 17 rue des Martyrs, 38054 Grenoble, France
[4] Micro Photon Devices S.r.l., via Antonio Stradivari 4, 39100 Bolzano, Italy
[5] Dipartimento di Elettronica, Informazione e Bioingegneria, Politecnico di Milano, piazza Leonardo da Vinci 32, 20133 Milano, Italy
[*] Corresponding author: dabac@fotonik.dtu.dk

Compiled October 5, 2018

The versatility of silicon photonic integrated circuits has led to a widespread usage of this platform for quantum information based applications, including Quantum Key Distribution (QKD). However, the integration of simple high repetition rate photon sources is yet to be achieved. The use of weak-coherent pulses (WCPs) could, in some cases, represent a viable solution. For example, Measurement Device Independent QKD (MDI-QKD) envisions the use of WCP to distill a secret key immune to detector side channel attacks at large distances. Thus, the integration of III-V lasers on silicon waveguides is an interesting prospect for quantum photonics. Here, we report the experimental observation of Hong-Ou-Mandel interference with $46 \pm 2\%$ visibility between WCPs generated by two independent III-V on silicon waveguide integrated lasers. This quantum interference effect is at the heart of many applications, including MDI-QKD. Our work, thus, represents a substantial first step towards an implementation of MDI-QKD fully integrated in silicon, and could be beneficial for other applications such as standard QKD and novel quantum communication protocols.

http://dx.doi.org/10.1364/ao.XX.XXXXXX

1. INTRODUCTION

Silicon photonic integrated circuits (PICs) are playing a major role on the development of quantum information based applications, such as quantum computation [1] and quantum communications [2]. Facilitated by the large variety of optical components available for integration [3], silicon PICs have been successfully designed to implement a variety of quantum protocols such as, multidimensional entanglement [4], high-dimensional Quantum Key Distribution (QKD) [5] and Quantum Random Number Generation [6]. However, challenges remain, in terms of scalability and losses, to fully integrate a simple high repetition rate photon source onto silicon PICs. A conceivable solution to this technical difficulty is to replace, when possible, single photons with weak coherent states (WCPs) generated by attenuating a laser pulse. Unfortunately, due to the indirect band gap of silicon, the development of a silicon laser remains an even greater challenge. To circumvent this, the integration of III-V sources on silicon PICs has been developed, offering promising prospects [7–9].

Quantum communication, whose goal is to outperform its classical counterpart in many communication tasks such as privacy, secrecy and authentication, could benefit from the use of silicon PICs and of the integration of III-V sources on such platform. In fact, silicon PICs would facilitate miniaturization and integration with existing telecommunications infrastructures. In particular, QKD, which can be securely implemented with WCPs using the decoy-state technique [10, 11], has been increasingly appealed by integrated photonic technologies [2, 12].

Despite the technical maturity of QKD, practical implementations are unavoidably imperfect, opening loopholes that can undermine the security of the protocol. A notorious example is the detector side channel attack, which can lead to the hacking of quantum cryptography systems [13]. To remove this vulnerability, Measurement-Device-Independent QKD (MDI-QKD) was introduced [14, 15], where a third untrusted party, i.e. Charlie, performs a Bell-state measurement on the WCPs sent by the two trusted parties, i.e. Alice and Bob, allowing them to establish a secure secret key based on time-revered entanglement [16]. Furthermore, this scheme has been used to distill secret keys between parties at record-setting distances [17]. However, to obtain a positive secret key rate, MDI-QKD requires high-visibility two-pulse interference between the WCPs sent by Alice and Bob [18].

The "bunching" of two indistinguishable photons that impinge on a beam-splitter, known as Hong-Ou-Mandel (HOM) interference [19], is a versatile quantum optics effect that has widespread application in quantum information based applications, for example, in the design of quantum logic circuits [20], in high precision time-deley measurements [21], and in quantum teleportation [22]. When the single photons are replaced with WCPs, HOM interference still occurs, but with a diminished visibility of 50% [23]. This effect is at the heart of MDI-QKD, since a high visibility of HOM interference is required for the successful distillation of the secure key. To obtain such visibility, the WCPs must be rendered highly indistinguishable, meaning that degrees of freedom, such as time-of-arrival, spectrum, polarization and mean number of photons per pulse, must be finely controlled and monitored.

In this letter, we report, for the first time, on the observation of high visibility HOM interference between WCPs generated by independent gain-switched III-V on silicon waveguide integrated lasers.

2. EXPERIMENTAL SETUP

A. Generation of WCPs from gain-switched III-V on silicon waveguide integrated lasers

The lasers used in this experiment were Distributed Feedback (DFB) based on Indium Phosphide heterogeneously integrated on silicon trough molecular wafer bonding, lasing linearly polarized light in the infrared *C*-band. This hybrid III-V on silicon technology was fabricated as described by Duan *et al.* [24].

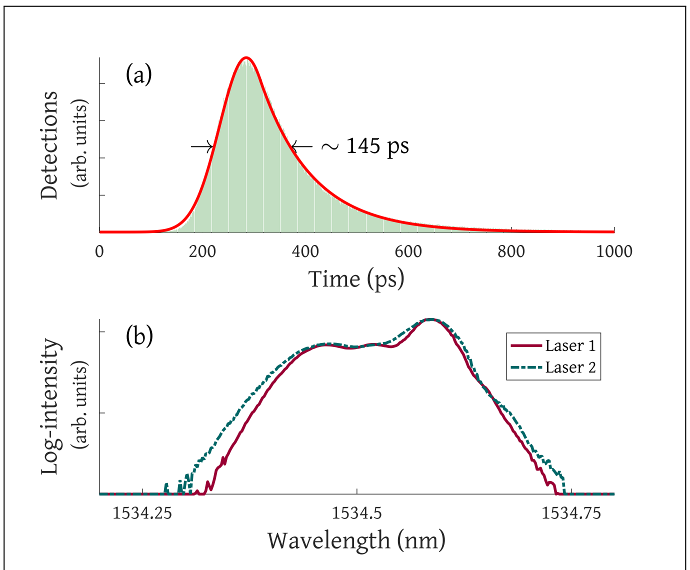

Fig. 1. Single photon detection temporal profile and spectral profile of the WCPs. **(a)** Detection histogram of the WCPs generated and detected as explained in 2.A. The solid line is obtained by fitting the experimental data with Eq. (1). Both laser emit pulses with equivalent detection temporal profiles with FWHM ≈ 145ps. **(b)** OSA trace of the laser pulses. Both lasers show similar spectral profiles centered at ∼1534.5nm and ∼400pm in width.

The lasers were independently probed and operated in gain-switching mode. This was realized by setting a bias current well below the lasing threshold, which is at ∼30mA, and sending an RF signal with repetition rate of 100MHz and ∼1ns electrical pulse duration generated by a Field Programmable Gate Array (FPGA). Operating the lasers in gain-switching mode generates short optical pulses with random phase, which is crucial for the security of QKD protocols [25]. A grating coupler in the silicon waveguide was used to couple the emitted light into single-mode optical fibers (SMFs). Fine tuning of the laser spectrum was performed by observing the emitted spectrum in an Optical Spectrum Analyzer (OSA) and by adjusting the temperature controller (TC) of the lasers. In figure 1 the measured temporal and spectral profiles of the obtained laser pulses can be observed.

From the spectral profiles, it is clear that the laser pulses are far from being transform limited. This is commonly observed in gain-switched semiconductor lasers, since the abrupt change in carrier density leads to a change in the refractive index of the active region, thus chirping the pulse [26]. Unfortunately, this chirp has a detrimental effect on the visibility of HOM interference. It therefore becomes necessary to use narrow bandpass filters to observe high visibility [27]. This was performed using a Santec OTF-350 tunable filter with 100pm bandpass (BPTF). The BPTF accounted for ∼10dB of loss, which does not represents a problem since WCPs with mean number of photons $\mu < 1$ are necessary to observe high-visibility HOM interference [23] and for MDI-QKD [18]. After being spectrally filtered, variable optical attenuators (VOA) are used to make WCPs with $\mu \approx 10^{-2}$.

The temporal profile of the single photon detection of the WCPs was obtained using a InGaAs/InP single-photon avalanche diode (SPAD) manufactured by Micro Photon Device S.r.l. [28] and the quTAG time-to-digital converter from qutools GmbH. The detector has a characteristic temporal response given by a Gaussian distribution followed by an exponential decay function:

$$Ae^{-\frac{(x-x_0)^2}{2\sigma^2}}\Theta(x_1-x) + Ae^{-\frac{(x_1-x_0)^2}{2\sigma^2}-\frac{x-x_1}{\tau}}\Theta(x-x_1) \tag{1}$$

where σ is the Gaussian standard deviation, x_0 is the Gaussian peak position, x_1 the crossover between Gaussian and exponential trend, τ is the exponential decay constant, $\Theta(x)$ is the Heaviside function and A is the Gaussian peak value. By fitting the data with Eq. (1), we calculate a full width at half maximum (FWHM) ≈ 145ps after spectral filtering. It is worth notice that this corresponds to the convolution between the response functions of the SPAD and of the time-to-digital converter with the temporal profile of the WCPs.

B. HOM interference Optical Setup

The optical setup used to observe HOM interference between WCPs generated by gain-switched III-V on silicon waveguide integrated lasers can be observed in figure 2. An optical delay-line (ODL) with micrometric precision was placed in the optical path of one to WCPs, allowing to match the time-of-arrival of the photons and to scan the HOM dip. Polarization controllers (PCs) were then placed to guarantee that the WCPs had identical polarizations. The WCPs from independent gain-switched III-V on silicon waveguide integrated lasers were then combined with a 50/50 beam-splitter (BS).

The output ports of the BS were connected to the SPADs operated at ∼100MHz gating regime with 3.5ns gate width. The dead-time of the detectors was set to 3μs and the bias voltage was set to 3.5V. These parameters allowed for an ideal compromise between intrinsic detector noise, mainly due to after pulses, and detection rate.

The detection events were then acquired by a time-to digital converter with temporal resolution of 81ps. A computer software was then used to generate detection histograms and to calculate coincidence rates and related quantities.

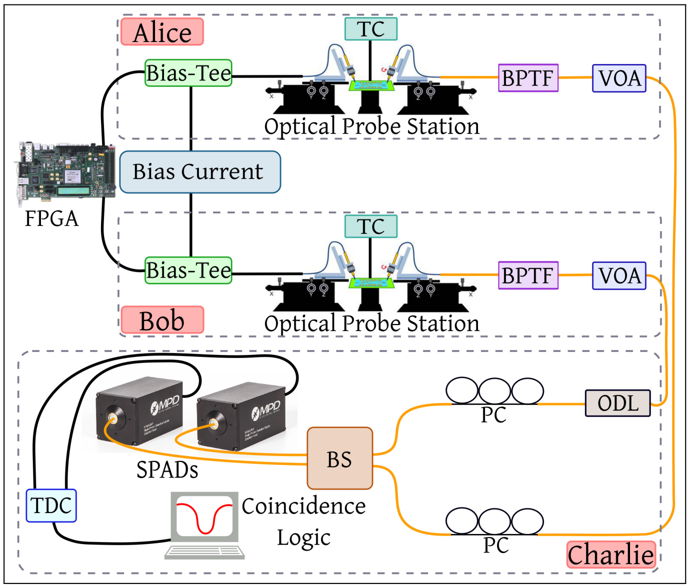

Fig. 2. Experimental setup to study HOM interference between WCPs generated by gain-switched III-V on silicon waveguide integrated lasers. For a detailed explanation see section 2. Black lines represent electrical connections while yellow lines represent optical connections via SMFs.

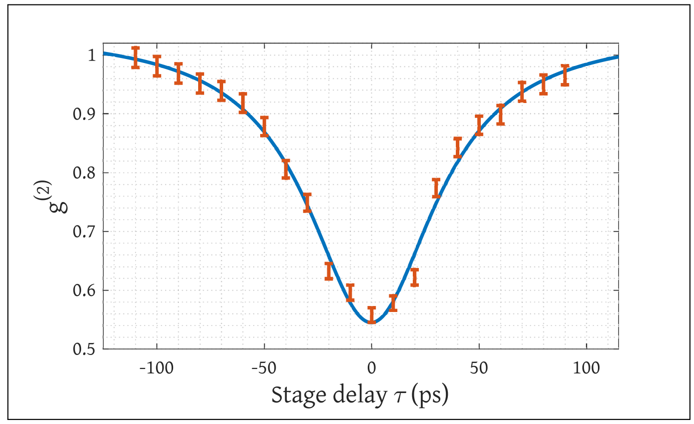

Fig. 3. HOM dip between WCPs generated by independent gain-switched III-V on silicon waveguide integrated lasers. The visibility, obtained by fitting the data with Eq. (3), is $\mathcal{V} = 46 \pm 2\%$.

3. RESULTS

A scan of the ODL was performed to observe HOM interference, recording all detection. From this data the value of the $g^{(2)}(\tau)$ intensity-intensity correlation was estimated as a function of the delay τ between the WCPs. The intensity-intensity correlation function, also known as the normalized coincidence rate, is defined as

$$g^{(2)} = \frac{P_{\text{Coinc}}}{P_{\text{D1}} P_{\text{D2}}} \tag{2}$$

where P_{Coinc} is the probability of measuring detection events in coincidence, and P_{D1}, P_{D1} are the detection probabilities for detectors 1 or 2 respectively. As the WCPs pass from being distinguishable due to the large difference in the time-of-arrival to being indistinguishable in all degrees of freedom, the $g^{(2)}(\tau)$ intensity-intensity correlation drops from 1 to a minimum of 0.5 in the ideal case. The dip follows a Lorentzian shape, and is of the form

$$g^{(2)}(\tau) = 1 - \mathcal{V}\frac{(\frac{\Gamma}{2})^2}{\tau^2 + (\frac{\Gamma}{2})^2} \tag{3}$$

where the observed visibility is $\mathcal{V}$, and Γ is the FWHM of the HOM dip.

In figure 3, the $g^{(2)}(\tau)$ intensity-intensity correlation is plotted as a function of the delay τ between the WCPs generated by independent gain-switched III-V on silicon waveguide integrated lasers. By fitting the data with Eq. (3), a visibility $\mathcal{V} = 46 \pm 2\%$ is estimated.

To provide a sensitive measure of the indistinguishably of the wavepackets of WCPs, a two-decoy experiment was recently proposed [29]. This allows to place an upper-bound on the probability $P(1,1|1,1)$ of a coincidence detection event given that only a single photon impinged on each input port of the BS, without any post-selection procedure. Such analysis can be of interest for QKD and for the analysis of quantum optics experiments using linear photonic circuits and WCPs. The upper-bound is given by

$$P(1,1|1,1)^{\text{ub}} = \frac{P^{\mu,\mu}_{\text{Coinc}} - P^{0,\mu}_{\text{Coinc}} - P^{\mu,0}_{\text{Coinc}}}{P_{\text{D1}} P_{\text{D2}}} \tag{4}$$

where $P^{\mu,\mu}_{\text{Coinc}}$ is the probability of a coincidence detection with mean average number of photons μ at each input port of the BS, $P^{0,\mu}_{\text{Coinc}}$ and $P^{\mu,0}_{\text{Coinc}}$ are the probabilities of a coincidence detection with the first, or second, BS input port blocked, and P_{D1}, P_{D1} are the detection probabilities for detectors 1 or 2 respectively without any blocked input port. Such analysis was performed and an upper bound of $P(1,1|1,1)^{\text{ub}} = 0.03 \pm 0.01$ was obtained at $\tau = 0$, deep within the quantum regime (i.e. $P(1,1|1,1)^{\text{ub}} < 0.5$).

4. DISCUSSION

In this letter we have reported, for the first time, HOM interference with visibility $\mathcal{V} = 46 \pm 2\%$ between two independent III-V on silicon waveguide integrated lasers. Such visibility is comparable with the visibility obtained in other HOM experiments between WCPs [17, 27, 30–32] and is sufficient to obtain a positive secret key rate in MDI-QKD [18].

Since each laser pulse is generated by spontaneous radiation with random phase, WCPs from gain-switched laser sources do not require further phase randomization. Furthermore, gain-switching operation generates short laser pulses, allowing for high repetition rates up to few GHz without the need of additional intensity modulators to carve the pulses. These characteristics simplify the complexity, and vastly reduces the amount of required optical components of a WCP generator.

It is worth noticing that both the bandpass filters and variable attenuators have already been integrated into silicon PICs [3, 8, 33]. Furthermore, since the fabrication of hybrid III-V on silicon lasers can be fully CMOS-compatible [34], envisioning a compact PIC which integrates all required components to generate WCPs exhibiting high-visibility HOM interference is a realistic short-term goal and is closer and closer to fulfill industrial requirements for mass production. Lastly, such WCP generator PIC could be further integrated into quantum state encoder PICs, using polarization or time-bin degrees of freedom [2], resulting in a compact silicon PIC capable of performing both MDI-QKD or standard QKD protocols such as BB84 [35].

A fully integrated WCP generator silicon PIC could also have interesting prospects in the practical implementation of novel quantum communication protocols based on WCPs and linear optics, such as quantum fingerprinting [36] and quantum appointment scheduling [37]. Furthermore, fully integrated WCPs generator PICs could be of interest for satellite quantum communications [38, 39] since such platform permits a small footprint, low energy consumptions, and resilience to vibrations and ionizing radiation. Lastly, this result paves the way for the implementation of metropolitan QKD networks based on silicon photonics [40] with fully integrated WCP sources.

FUNDING

This work is supported by the Center of Excellence, SPOC-Silicon Photonics for Optical Communications (ref DNRF123), by the People Programme (Marie Curie Actions) of the European Union's Seventh Framework Programme (FP7/2007-2013) under REA grant agreement n° 609405 (COFUNDPostdocDTU) and by QuantERA ERA-NET SQUARE project.

ACKNOWLEDGMENTS

During the preparation of this letter, the authors became aware of similar work by H. Semenenko, et al. using Indium Phosphide gain switched lasers to demonstrate HOM interference [41]. We thank S. Paesani for the fruitful discussions. C.A. acknowledges financial support from the COST action MP1403 "Nanoscale Quantum Optic".

REFERENCES

1. A. Peruzzo, J. McClean, P. Shadbolt, M. H. Yung, X. Q. Zhou, P. J. Love, A. Aspuru-Guzik, and J. L. O'Brien, Nat. Commun. **5**, 4213 (2014).
2. P. Sibson, J. E. Kennard, S. Stanisic, C. Erven, J. L. O'Brien, and M. G. Thompson, Optica. **4**, 172 (2017).
3. B. Jalali and S. Fathpour, J. Light. Technol. **24**, 4600 (2006).
4. J. Wang, S. Paesani, Y. Ding, R. Santagati, P. Skrzypczyk, A. Salavrakos, J. Tura, R. Augusiak, L. Mančinska, D. Bacco, D. Bonneau, J. W. Silverstone, Q. Gong, A. Acín, K. Rottwitt, L. K. Oxenløwe, J. L. O'Brien, A. Laing, and M. G. Thompson, Science. **360**, 285 (2018).
5. Y. Ding, D. Bacco, K. Dalgaard, X. Cai, X. Zhou, K. Rottwitt, and L. K. Oxenløwe, npj Quantum Inf. **3**, 25 (2017).
6. F. Raffaelli, G. Ferranti, D. H. Mahler, P. Sibson, J. E. Kennard, A. Santamato, G. Sinclair, D. Bonneau, M. G. Thompson, and J. C. F. Matthews, Quantum Sci. Technol. **3**, 025003 (2018).
7. P. Kaspar, C. Jany, A. Le Liepvre, A. Accard, M. Lamponi, D. Make, G. Levaufre, N. Girard, F. Lelarge, A. Shen, P. Charbonnier, F. Mallecot, G.-H. Duan, J. . Gentner, J.-M. Fedeli, S. Olivier, A. Descos, B. Ben Bakir, S. Messaoudene, D. Bordel, S. Malhouitre, C. Kopp, and S. Menezo, "Hybrid III-V/silicon lasers," in *SPIE Silicon Photonics Photonics Integr. Circuits IV,* , vol. 9133 L. Vivien, S. Honkanen, L. Pavesi, S. Pelli, and J. H. Shin, eds. (International Society for Optics and Photonics, 2014), p. 913302.
8. V. Cristofori, F. Da Ros, O. Ozolins, M. E. Chaibi, L. Bramerie, Y. Ding, X. Pang, A. Shen, A. Gallet, G.-H. Duan, K. Hassan, S. Olivier, S. Popov, G. Jacobsen, L. K. Oxenløwe, and C. Peucheret, IEEE Photonics Technol. Lett. **29**, 960 (2017).
9. X. Wang, C. Ma, R. Kumar, P. Doussiere, R. Jones, H. Rong, and S. Mookherjea, APL Photonics **3**, 106104 (2018).
10. X.-B. Wang, Phys. Rev. Lett. **94**, 230503 (2005).
11. H.-K. Lo, X. Ma, and K. Chen, Phys. Rev. Lett. **94**, 230504 (2005).
12. P. Sibson, C. Erven, M. Godfrey, S. Miki, T. Yamashita, M. Fujiwara, M. Sasaki, H. Terai, M. G. Tanner, C. M. Natarajan, R. H. Hadfield, J. L. O'Brien, and M. G. Thompson, Nat. Commun. **8**, 13984 (2017).
13. L. Lydersen, C. Wiechers, C. Wittmann, D. Elser, J. Skaar, and V. Makarov, Nat. Photonics **4**, 686 (2010).
14. S. L. Braunstein and S. Pirandola, Phys. Rev. Lett. **108**, 130502 (2012).
15. H.-K. Lo, M. Curty, and B. Qi, Phys. Rev. Lett. **108**, 130503 (2012).
16. H. Inamori, Algorithmica. **34**, 340 (2002).
17. H.-L. Yin, T.-Y. Chen, Z.-W. Yu, H. Liu, L.-X. You, Y.-H. Zhou, S.-J. Chen, Y. Mao, M.-Q. Huang, W.-J. Zhang, H. Chen, M. J. Li, D. Nolan, F. Zhou, X. Jiang, Z. Wang, Q. Zhang, X.-B. Wang, and J.-W. Pan, Phys. Rev. Lett. **117**, 190501 (2016).
18. F. Xu, M. Curty, B. Qi, and H.-K. Lo, New J. Phys. **15**, 113007 (2013).
19. C. K. Hong, Z. Y. Ou, and L. Mandel, Phys. Rev. Lett. **59**, 2044 (1987).
20. P. Kok, W. J. Munro, K. Nemoto, T. C. Ralph, J. P. Dowling, and G. J. Milburn, Rev. Mod. Phys. **79**, 135 (2007).
21. A. Lyons, G. C. Knee, E. Bolduc, T. Roger, J. Leach, E. M. Gauger, and D. Faccio, Sci. Adv. **4**, eaap9416 (2018).
22. R. Valivarthi, M. G. Puigibert, Q. Zhou, G. H. Aguilar, V. B. Verma, F. Marsili, M. D. Shaw, S. W. Nam, D. Oblak, and W. Tittel, Nat. Photonics **10**, 676 (2016).
23. E. Moschandreou, J. I. Garcia, B. J. Rollick, B. Qi, R. Pooser, and G. Siopsis, J. Light. Technol. **36**, 3752 (2018).
24. G.-H. Duan, C. Jany, A. Le Liepvre, A. Accard, M. Lamponi, D. Make, P. Kaspar, G. Levaufre, N. Girard, F. Lelarge, J.-M. Fedeli, A. Descos, B. Ben Bakir, S. Messaoudene, D. Bordel, S. Menezo, G. de Valicourt, S. Keyvaninia, G. Roelkens, D. Van Thourhout, D. J. Thomson, F. Y. Gardes, and G. T. Reed, IEEE J. Sel. Top. Quantum Electron. **20**, 158 (2014).
25. T. Kobayashi, A. Tomita, and A. Okamoto, Phys. Rev. A **90**, 032320 (2014).
26. D. Welford, IEEE J. Quantum Electron. **21**, 1749 (1985).
27. Z. L. Yuan, M. Lucamarini, J. F. Dynes, B. Fröhlich, M. B. Ward, and A. J. Shields, Phys. Rev. Appl. **2**, 064006 (2014).
28. A. Tosi, A. Della Frera, A. Bahgat Shehata, and C. Scarcella, Rev. Sci. Instrum. **83**, 013104 (2012).
29. A. Aragoneses, N. T. Islam, M. Eggleston, A. Lezama, J. Kim, and D. J. Gauthier, Opt. Lett. **43**, 3806 (2018).
30. A. Rubenok, J. A. Slater, P. Chan, I. Lucio-Martinez, and W. Tittel, Phys. Rev. Lett. **130501**, 1 (2013).
31. Z. Tang, Z. Liao, F. Xu, B. Qi, L. Qian, and H.-K. Lo, Phys. Rev. Lett. **112**, 190503 (2014).
32. M. Namazi, M. Flament, A. Scriminich, S. Gera, S. Sagona-Stophel, G. Vallone, P. Villoresi, and E. Figueroa, arXiv. (2018).
33. M. Piekarek, D. Bonneau, S. Miki, T. Yamashita, M. Fujiwara, M. Sasaki, H. Terai, M. G. Tanner, C. M. Natarajan, R. H. Hadfield, J. L. O'Brien, and M. G. Thompson, Opt. Lett. **42**, 815 (2017).
34. B. Szelag, K. Hassan, L. Adelmini, E. Ghegin, P. Rodriguez, S. Bensalem, F. Nemouchi, T. Bria, M. Brihoum, P. Brianceau, E. Vermande, O. Pesenti, A. Schembri, R. Crochemore, S. Dominguez, M. C. Roure, B. Montmayeul, L. Sanchez, and C. Jany, "Hybrid III-V/Si DFB laser integration on a 200 mm fully CMOS-compatible silicon photonics platform," in *2017 IEEE International Electron Devices Meeting (IEDM),* (IEEE, 2017), pp. 24.1.1–24.1.4.
35. C. H. Bennett and G. Brassard, Theor. Comput. Sci. **560**, 7 (2014).
36. J. M. Arrazola and N. Lütkenhaus, Phys. Rev. A **89**, 062305 (2014).
37. D. Touchette, B. Lovitz, and N. Lütkenhaus, Phys. Rev. A **97**, 042320 (2018).
38. D. K. Oi, A. Ling, G. Vallone, P. Villoresi, S. Greenland, E. Kerr, M. Macdonald, H. Weinfurter, H. Kuiper, E. Charbon, and R. Ursin, EPJ Quantum Technol. **4**, 6 (2017).
39. C. Agnesi, F. Vedovato, M. Schiavon, D. Dequal, L. Calderaro, M. Tomasin, D. G. Marangon, A. Stanco, V. Luceri, G. Bianco, G. Vallone, and P. Villoresi, Philos. Trans. R. Soc. Lond. Ser. A Math. Phys. Eng. Sci. **376**, 20170461 (2018).
40. D. Bunandar, A. Lentine, C. Lee, H. Cai, C. M. Long, N. Boynton, N. Martinez, C. Derose, C. Chen, M. Grein, D. Trotter, A. Starbuck, A. Pomerene, S. Hamilton, F. N. C. Wong, R. Camacho, P. Davids, J. Urayama, and D. Englund, Phys. Rev. X **8**, 021009 (2018).
41. H. Semenenko, P. Sibson, M. G. Thomson, and C. Erven, Opt. Lett. (2018).

FULL REFERENCES

1. A. Peruzzo, J. McClean, P. Shadbolt, M. H. Yung, X. Q. Zhou, P. J. Love, A. Aspuru-Guzik, and J. L. O'Brien, "A variational eigenvalue solver on a photonic quantum processor," Nat. Commun. **5**, 4213 (2014).
2. P. Sibson, J. E. Kennard, S. Stanisic, C. Erven, J. L. O'Brien, and M. G. Thompson, "Integrated silicon photonics for high-speed quantum key distribution," Optica. **4**, 172 (2017).
3. B. Jalali and S. Fathpour, "Silicon Photonics," J. Light. Technol. **24**, 4600–4615 (2006).
4. J. Wang, S. Paesani, Y. Ding, R. Santagati, P. Skrzypczyk, A. Salavrakos, J. Tura, R. Augusiak, L. Mančinska, D. Bacco, D. Bonneau, J. W. Silverstone, Q. Gong, A. Acín, K. Rottwitt, L. K. Oxenløwe, J. L. O'Brien, A. Laing, and M. G. Thompson, "Multidimensional quantum entanglement with large-scale integrated optics," Science. **360**, 285–291 (2018).
5. Y. Ding, D. Bacco, K. Dalgaard, X. Cai, X. Zhou, K. Rottwitt, and L. K. Oxenløwe, "High-dimensional quantum key distribution based on multicore fiber using silicon photonic integrated circuits," npj Quantum Inf. **3**, 25 (2017).
6. F. Raffaelli, G. Ferranti, D. H. Mahler, P. Sibson, J. E. Kennard, A. Santamato, G. Sinclair, D. Bonneau, M. G. Thompson, and J. C. F. Matthews, "A homodyne detector integrated onto a photonic chip for measuring quantum states and generating random numbers," Quantum Sci. Technol. **3**, 025003 (2018).
7. P. Kaspar, C. Jany, A. Le Liepvre, A. Accard, M. Lamponi, D. Make, G. Levaufre, N. Girard, F. Lelarge, A. Shen, P. Charbonnier, F. Mallecot, G.-H. Duan, J. . Gentner, J.-M. Fedeli, S. Olivier, A. Descos, B. Ben Bakir, S. Messaoudene, D. Bordel, S. Malhouitre, C. Kopp, and S. Menezo, "Hybrid III-V/silicon lasers," in *SPIE Silicon Photonics Photonics Integr. Circuits IV,* , vol. 9133 L. Vivien, S. Honkanen, L. Pavesi, S. Pelli, and J. H. Shin, eds. (International Society for Optics and Photonics, 2014), p. 913302.
8. V. Cristofori, F. Da Ros, O. Ozolins, M. E. Chaibi, L. Bramerie, Y. Ding, X. Pang, A. Shen, A. Gallet, G.-H. Duan, K. Hassan, S. Olivier, S. Popov, G. Jacobsen, L. K. Oxenløwe, and C. Peucheret, "25-Gb/s Transmission Over 2.5-km SSMF by Silicon MRR Enhanced 1.55- μm III-V/SOI DML," IEEE Photonics Technol. Lett. **29**, 960–963 (2017).
9. X. Wang, C. Ma, R. Kumar, P. Doussiere, R. Jones, H. Rong, and S. Mookherjea, "Photon pair generation using a silicon photonic hybrid laser," APL Photonics **3**, 106104 (2018).
10. X.-B. Wang, "Beating the Photon-Number-Splitting Attack in Practical Quantum Cryptography," Phys. Rev. Lett. **94**, 230503 (2005).
11. H.-K. Lo, X. Ma, and K. Chen, "Decoy State Quantum Key Distribution," Phys. Rev. Lett. **94**, 230504 (2005).
12. P. Sibson, C. Erven, M. Godfrey, S. Miki, T. Yamashita, M. Fujiwara, M. Sasaki, H. Terai, M. G. Tanner, C. M. Natarajan, R. H. Hadfield, J. L. O'Brien, and M. G. Thompson, "Chip-based quantum key distribution," Nat. Commun. **8**, 13984 (2017).
13. L. Lydersen, C. Wiechers, C. Wittmann, D. Elser, J. Skaar, and V. Makarov, "Hacking commercial quantum cryptography systems by tailored bright illumination," Nat. Photonics **4**, 686–689 (2010).
14. S. L. Braunstein and S. Pirandola, "Side-Channel-Free Quantum Key Distribution," Phys. Rev. Lett. **108**, 130502 (2012).
15. H.-K. Lo, M. Curty, and B. Qi, "Measurement-Device-Independent Quantum Key Distribution," Phys. Rev. Lett. **108**, 130503 (2012).
16. H. Inamori, "Security of Practical Time-Reversed EPR Quantum Key Distribution," Algorithmica. **34**, 340–365 (2002).
17. H.-L. Yin, T.-Y. Chen, Z.-W. Yu, H. Liu, L.-X. You, Y.-H. Zhou, S.-J. Chen, Y. Mao, M.-Q. Huang, W.-J. Zhang, H. Chen, M. J. Li, D. Nolan, F. Zhou, X. Jiang, Z. Wang, Q. Zhang, X.-B. Wang, and J.-W. Pan, "Measurement-Device-Independent Quantum Key Distribution Over a 404 km Optical Fiber," Phys. Rev. Lett. **117**, 190501 (2016).
18. F. Xu, M. Curty, B. Qi, and H.-K. Lo, "Practical aspects of measurement-device-independent quantum key distribution," New J. Phys. **15**, 113007 (2013).
19. C. K. Hong, Z. Y. Ou, and L. Mandel, "Measurement of subpicosecond time intervals between two photons by interference," Phys. Rev. Lett. **59**, 2044–2046 (1987).
20. P. Kok, W. J. Munro, K. Nemoto, T. C. Ralph, J. P. Dowling, and G. J. Milburn, "Linear optical quantum computing with photonic qubits," Rev. Mod. Phys. **79**, 135–174 (2007).
21. A. Lyons, G. C. Knee, E. Bolduc, T. Roger, J. Leach, E. M. Gauger, and D. Faccio, "Attosecond-resolution Hong-Ou-Mandel interferometry," Sci. Adv. **4**, eaap9416 (2018).
22. R. Valivarthi, M. G. Puigibert, Q. Zhou, G. H. Aguilar, V. B. Verma, F. Marsili, M. D. Shaw, S. W. Nam, D. Oblak, and W. Tittel, "Quantum teleportation across a metropolitan fibre network," Nat. Photonics **10**, 676–680 (2016).
23. E. Moschandreou, J. I. Garcia, B. J. Rollick, B. Qi, R. Pooser, and G. Siopsis, "Experimental Study of Hong-Ou-Mandel Interference Using Independent Phase Randomized Weak Coherent States," J. Light. Technol. **36**, 3752–3759 (2018).
24. G.-H. Duan, C. Jany, A. Le Liepvre, A. Accard, M. Lamponi, D. Make, P. Kaspar, G. Levaufre, N. Girard, F. Lelarge, J.-M. Fedeli, A. Descos, B. Ben Bakir, S. Messaoudene, D. Bordel, S. Menezo, G. de Valicourt, S. Keyvaninia, G. Roelkens, D. Van Thourhout, D. J. Thomson, F. Y. Gardes, and G. T. Reed, "Hybrid III–V on Silicon Lasers for Photonic Integrated Circuits on Silicon," IEEE J. Sel. Top. Quantum Electron. **20**, 158–170 (2014).
25. T. Kobayashi, A. Tomita, and A. Okamoto, "Evaluation of the phase randomness of a light source in quantum-key-distribution systems with an attenuated laser," Phys. Rev. A **90**, 032320 (2014).
26. D. Welford, "A rate equation analysis for the frequency chirp to modulated power ratio of a semiconductor diode laser," IEEE J. Quantum Electron. **21**, 1749–1751 (1985).
27. Z. L. Yuan, M. Lucamarini, J. F. Dynes, B. Fröhlich, M. B. Ward, and A. J. Shields, "Interference of Short Optical Pulses from Independent Gain-Switched Laser Diodes for Quantum Secure Communications," Phys. Rev. Appl. **2**, 064006 (2014).
28. A. Tosi, A. Della Frera, A. Bahgat Shehata, and C. Scarcella, "Fully programmable single-photon detection module for InGaAs/InP single-photon avalanche diodes with clean and sub-nanosecond gating transitions," Rev. Sci. Instrum. **83**, 013104 (2012).
29. A. Aragoneses, N. T. Islam, M. Eggleston, A. Lezama, J. Kim, and D. J. Gauthier, "Bounding the outcome of a two-photon interference measurement using weak coherent states," Opt. Lett. **43**, 3806 (2018).
30. A. Rubenok, J. A. Slater, P. Chan, I. Lucio-Martinez, and W. Tittel, "Real-World Two-Photon Interference and Proof-of-Principle Quantum Key Distribution Immune to Detector Attacks," Phys. Rev. Lett. **130501**, 1–5 (2013).
31. Z. Tang, Z. Liao, F. Xu, B. Qi, L. Qian, and H.-K. Lo, "Experimental Demonstration of Polarization Encoding Measurement-Device-Independent Quantum Key Distribution," Phys. Rev. Lett. **112**, 190503 (2014).
32. M. Namazi, M. Flament, A. Scriminich, S. Gera, S. Sagona-Stophel, G. Vallone, P. Villoresi, and E. Figueroa, "A multi-node room-temperature quantum network," arXiv. (2018).
33. M. Piekarek, D. Bonneau, S. Miki, T. Yamashita, M. Fujiwara, M. Sasaki, H. Terai, M. G. Tanner, C. M. Natarajan, R. H. Hadfield, J. L. O'Brien, and M. G. Thompson, "High-extinction ratio integrated photonic filters for silicon quantum photonics," Opt. Lett. **42**, 815 (2017).
34. B. Szelag, K. Hassan, L. Adelmini, E. Ghegin, P. Rodriguez, S. Bensalem, F. Nemouchi, T. Bria, M. Brihoum, P. Brianceau, E. Vermande, O. Pesenti, A. Schembri, R. Crochemore, S. Dominguez, M. C. Roure, B. Montmayeul, L. Sanchez, and C. Jany, "Hybrid III-V/Si DFB laser integration on a 200 mm fully CMOS-compatible silicon photonics platform," in *2017 IEEE International Electron Devices Meeting (IEDM),* (IEEE, 2017), pp. 24.1.1–24.1.4.
35. C. H. Bennett and G. Brassard, "Quantum cryptography: Public key distribution and coin tossing," Theor. Comput. Sci. **560**, 7–11 (2014).
36. J. M. Arrazola and N. Lütkenhaus, "Quantum fingerprinting with coherent states and a constant mean number of photons," Phys. Rev. A **89**, 062305 (2014).
37. D. Touchette, B. Lovitz, and N. Lütkenhaus, "Practical quantum appointment scheduling," Phys. Rev. A **97**, 042320 (2018).
38. D. K. Oi, A. Ling, G. Vallone, P. Villoresi, S. Greenland, E. Kerr, M. Mac-

donald, H. Weinfurter, H. Kuiper, E. Charbon, and R. Ursin, "CubeSat quantum communications mission," EPJ Quantum Technol. **4**, 6 (2017).
39. C. Agnesi, F. Vedovato, M. Schiavon, D. Dequal, L. Calderaro, M. Tomasin, D. G. Marangon, A. Stanco, V. Luceri, G. Bianco, G. Vallone, and P. Villoresi, "Exploring the boundaries of quantum mechanics: advances in satellite quantum communications," Philos. Trans. R. Soc. Lond. Ser. A Math. Phys. Eng. Sci. **376**, 20170461 (2018).
40. D. Bunandar, A. Lentine, C. Lee, H. Cai, C. M. Long, N. Boynton, N. Martinez, C. Derose, C. Chen, M. Grein, D. Trotter, A. Starbuck, A. Pomerene, S. Hamilton, F. N. C. Wong, R. Camacho, P. Davids, J. Urayama, and D. Englund, "Metropolitan Quantum Key Distribution with Silicon Photonics," Phys. Rev. X **8**, 021009 (2018).
41. H. Semenenko, P. Sibson, M. G. Thomson, and C. Erven, "Interference between independent photonic integrated devices for quantum key distribution," Opt. Lett. (2018).